

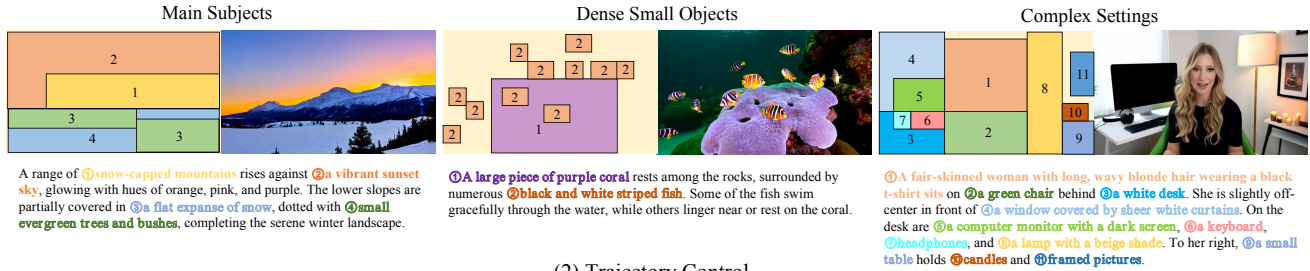
InstanceV: Instance-Level Video Generation

Yuheng Chen¹ Teng Hu¹ Jiangning Zhang² Zhucun Xue² Ran Yi¹
Lizhuang Ma^{1†}

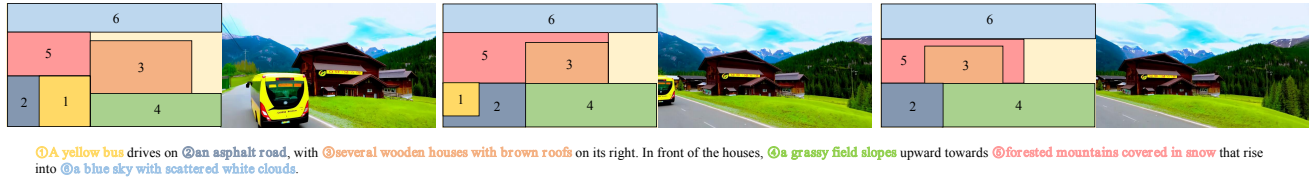
¹Shanghai Jiao Tong University ²Zhejiang University

Project page: <https://aliiothchen.github.io/projects/InstanceV>

(1) Layout and Feature Control



(2) Trajectory Control



(3) Camera Control

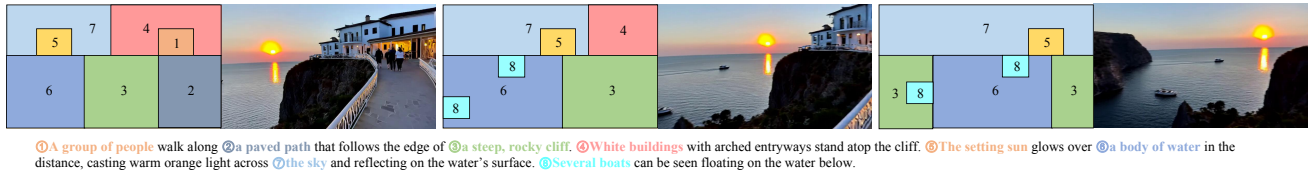


Figure 1. The instance-level grounding information not only helps the video diffusion model better understand fine-grained control cues in the global video caption, such as instances layout and attributes, but also enables indirect realization of instance-level trajectory control and global camera motion control.

Abstract

Recent advances in text-to-video diffusion models have enabled the generation of high-quality videos conditioned on textual descriptions. However, most existing text-to-video models rely solely on textual conditions, lacking general fine-grained controllability over video generation. To address this challenge, we propose **InstanceV**, a video generation framework that enables **i)** instance-level control and **ii)** global semantic consistency. Specifically, with the aid of proposed Instance-aware Masked Cross-Attention mechanism, InstanceV maximizes the utilization of addi-

tional instance-level grounding information to generate correctly attributed instances at designated spatial locations. To improve overall consistency, We introduce the Shared Timestep-Adaptive Prompt Enhancement module, which connects local instances with global semantics in a parameter-efficient manner. Furthermore, we incorporate Spatially-Aware Unconditional Guidance during both training and inference to alleviate the disappearance of small instances. Finally, we propose a new benchmark, named InstanceBench, which combines general video quality metrics with instance-aware metrics for more comprehensive evaluation on instance-level video generation. Extensive experiments demonstrate that InstanceV not only achieves remarkable instance-level controllability in video

[†] Corresponding author.

generation, but also outperforms existing state-of-the-art models in both general quality and instance-aware metrics across qualitative and quantitative evaluations.

1. Introduction

Driven by rapid advances in foundational backbones [29] and multimodal interaction, a new generation of open-source [4, 24, 38, 47] has been introduced. These models not only substantially improve the visual quality, text-to-video cross-modal alignment and diversity of generated videos, but also demonstrate promising applications in real-world scenarios like education, design, and entertainment.

However, existing video generation frameworks share a notable limitation: they struggle to maintain fidelity to complex prompts, particularly those specifying multiple interacting instances or intricate spatial relationships. This limitation often manifests as semantic errors, such as missing instances or misattributed properties, and may result in noticeable visual artifacts in the generated videos. Prior to the recent focus on video generation, extensive research in text-to-image (T2I) synthesis explored methods for fine-grained instance-level control, which can be broadly divided into three types, (1) *Implicitly conditioned methods* [25, 40, 52] treat instance-level grounding information as additional visual tokens, which are injected through a residual self-attention mechanism. Such methods require resource-intensive training, making them computationally prohibitive for most open-source video diffusion models. (2) *First-instances-then-merge* [40, 54] methods generate each instance separately before merging them together. These methods often require more denoising steps, and temporal consistencies are challenging to preserve in such manner. (3) *Training-free* [34] approaches directly manipulate attention maps during inference. These methods pose significant challenges to current GPU hardware, as larger video feature maps result in substantially larger attention maps.

To address these challenges, we propose **InstanceV**, a computationally efficient and training-efficient video generation framework. Specifically, we propose an **Instance-aware Masked Cross-Attention (IMCA)** module that seamlessly integrates instance-level grounding information into the backbone, serving as an explicit guidance signal for the native cross-attention. IMCA enables the synthesis of objects with specified attributes at desired spatial locations without additional denoising steps, while remaining computationally lightweight and easy to train. To maintain global semantic consistency and temporal coherence, we further design a **Shared Timestep-Adaptive Prompt Enhancement (STAPE)** module, which effectively bridges local instance semantics with the global video caption in a parameter-efficient manner. Furthermore, we incorporate a **Spatially-Aware Unconditional Guidance (SAUG)** strat-

egy in both training and inference. By leaving the instance prompts empty, this mechanism encourages the model to better reason about spatial relationships among instances, thereby refining the generation of smaller instances. Finally, to better evaluate instance-level video generation, we propose a comprehensive benchmark named InstanceBench, which consists of both general video quality and instance-level evaluation metrics for a more holistic assessment.

We conduct extensive experiments by extending the Wan-series [38] models with our proposed InstanceV framework. Comparison against leading state-of-the-art models, including Wan-series, HunyuanVideo [24], CogVideoX [47], and SkyReelsV2 [4], demonstrate that *InstanceV* surpasses all competing models on InstanceBench, showing superior performance on both general video quality metrics and specialized instance-aware metrics. Our main contributions are fourfold:

- We propose InstanceV, a computationally efficient yet powerful video generation framework and, to the best of our knowledge, the first to be designed specifically for instance-level control at the architectural level.
- We introduce Instance-aware Masked Cross-Attention, which explicitly associates instance-level prompts with their corresponding visual tokens, thereby enabling the precise and reliable generation of correct spatial layouts and richly detailed instance-specific attributes.
- We present a Shared Timestep-Adaptive Prompt Enhancement module to effectively mitigate potential semantic inconsistencies. Furthermore, we substantially enhance small-instance generation by incorporating a Spatially-Aware Unconditional Guidance strategy.
- To facilitate rigorous and comprehensive evaluation, we introduce InstanceBench, a new benchmark specifically designed for instance-level video generation.

2. Related Works

2.1. Video Diffusion Foundation Models

Driven by rapid advances in generative modeling, diffusion-based frameworks [17, 19, 20, 53] have become the widely adopted architecture for video generation, among which DiT [29] plays a central role owing to its outstanding scalability. Recent models, such as the Wan series [38] and HunyuanVideo [24], further extend DiT and achieve impressive video generation performance through large-scale training on high-quality text-video datasets. Nevertheless, these models struggle when confronted with complex video captions depicting multiple interacting instances and intricate spatial relationships.

2.2. Controllable Video Diffusion

Several existing works have sought to extend the grounding information of video diffusion from diverse perspec-

Method	FLOPS ↓	Params ↓	Time Cost ↓
GLIGEN [25]	102.79%	26.13%	96.83%
InstanceDiffusion [40]	121.82%	42.94%	115.69%
InstanceGen [34]	40.00%	—	80.00%
InstanceV(ours)	15.02%	20.65%	9.14%

Table 1. Additional FLOPs, parameters, and time overhead (%) introduced for instance-level control relative to the backbone.

tives, including general conditional controls such as camera [1, 11], motion [3, 28], audio [5, 39], and trajectory [44, 50], as well as subject- and id-preserving controls [18, 48] that focus on humans or other specific entities. These approaches typically require the acquisition of specific control conditions, which are subsequently injected into the diffusion backbone via additional modules. Consequently, many of them are heavily dependent on large-scale, high-quality, task-specific training data [11, 39, 44], and the increased structural complexity of the specialized modules [3, 39] further limits effective training and generalization. Furthermore, the generated content conditioned on certain grounding information remains highly constrained [28], whereas subject- and id-preserving approaches [18, 48] primarily focus on controlling larger instances. Notably, some works aim to unify multiple formats of grounding information within a single framework. For instance, VACE [23] introduces a Video Condition Unit (VCU) for task-agnostic control, while DaS [11] leverages 3D-tracked videos for generation, treating 2D videos as projections of 3D content. In contrast, InstanceV achieves a simple yet effective form of instance-level control according to Table 1, which also extends naturally to support a broader range of control types.

2.3. Instance-Level Control

For text-to-image generation, several instance-level control methods have been proposed. CLIGEN [25] serves as an early pioneer in this line of work, which fuses instance features and spatial locations via neural networks and injects them into the backbone through a residual self-attention module. InstanceDiffusion [40] extends CLIGEN by enriching the forms of injected spatial configurations. MIGC [54] features generating each instance independently followed by subsequent fusions. LayoutDiffusion [52] maps visual tokens and instance information into a shared latent space to facilitate more effective interaction. In addition, InstanceGen [34] manipulates the generation process by reweighting and masking attention maps during inference. For text-to-video tasks, InstanceCap [7] represents the first attempt from a data-driven perspective, introducing an instance-level dataset annotated by a proposed instance-aware captioner. Compared to above works, InstanceV is more lightweight and computationally efficient, achieving more direct instance-level control benefited from a specialized model design.

3. Instance-Level Data Preparation

To allow for richer instance-level information injection, we design a data preprocessing pipeline that extracts the most accurate instance information possible from existing text–video pairs.

3.1. MLLM-based Instance Partitioning

Foreground. To obtain both semantic and spatial information of different foreground instances, we adopt the *Florence-2* [43] together with *Grounded-Sam2* [31, 32], and the pipeline proceeds as follows: **(1)** We first utilize the phrase grounding segmentation task to initially identify the textual prompts and spatial locations of individual instances. **(2)** We then integrate the outputs from more tasks, such as object detection, to obtain more accurate and comprehensive instance segmentation results. Two limitations remain in the previous results: 1) when multiple objects with similar semantics appear (e.g., “a crowd of people”), *Florence-2* tends to merge them into a single large instance, resulting in ambiguous semantic representations; and 2) large instances that are partially occluded by other objects may be completely missed. By integrating the complementary outputs from different tasks, more accurate and complete instance-level grounding information can be obtained. **(3)** We further employ a CLIPScore-based [30] filtering strategy to prune potentially erroneous instance segmentations. Unlike static images, videos naturally exhibit temporal variations, where certain instances may newly appear or disappear across frames. Using the same text description to process all frames can therefore lead to mislabeling. The CLIPScore-based filtering helps mitigate such problems by removing mismatched instances.

Background. To facilitate a more straightforward and coherent implementation of InstanceV, we utilize a background prompt derived from the summarized video caption by an LLM [46] as the instance information for regions not associated with any specific foreground instances. At this stage, the instance-level grounding information includes textual instance prompts and spatial coordinates in the form of bounding boxes. Please refer to Section 4 and the supplementary materials for details on how these are converted into model inputs.

3.2. Downscale and Patchifying

In mainstream video diffusion models, videos are represented as discrete visual tokens obtained through a VAE and a patchifying module, where both spatial and temporal dimensions are compressed. Spatially, the bounding boxes can be directly rescaled. Temporally, let T_{ds} denote the temporal downscaling factor of the VAE. Assuming 0-indexing, we extract additional grounding information only from frames $(0, T_{ds}, 2T_{ds}, \dots)$. This design relies on the assumption that within a short temporal stride, the number

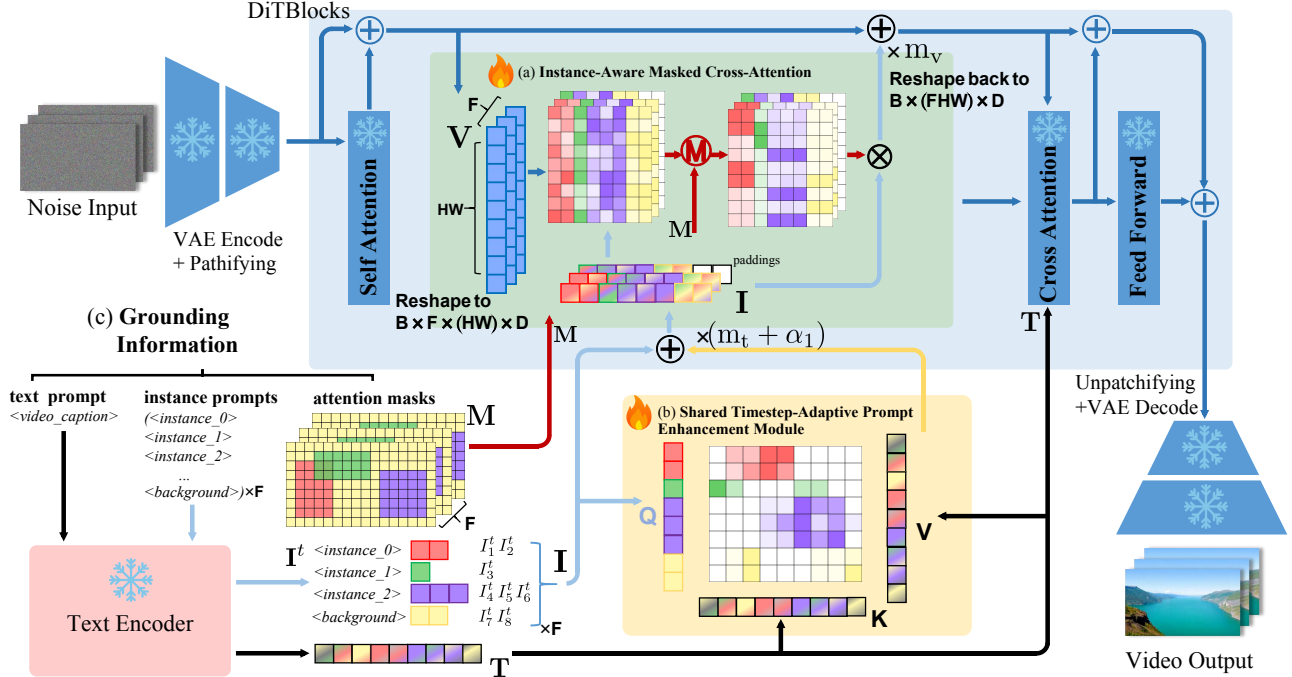


Figure 2. Overview of the proposed InstanceV framework. (a) Only a small subset of visual tokens is shown due to space limitations; this visualization can be interpreted as a case where $H = 1$. (b) Solid colors denote independently encoded instance prompts, while the tokens with color encode more global semantic information. (c) The grounding information consists of F groups of attention masks and instance prompts, where the instances differ across frames due to temporal variation. Note that for simplicity, the attention masks are drawn as $F \times H \times W$, with colors distinguishing different instances.

and spatial distribution of instances remain relatively stable. Such a strategy reduces the computational overhead of data preprocessing, simplifies the model complexity, and allows for more straightforward injection of instance-level grounding information.

4. Methods

To enable instance-level control, we make *three key modifications* to the DiT backbone. First, by introducing the **Instance-aware Masked Cross-Attention (IMCA)**, instance-level grounding information is efficiently injected into the model, guiding the cross-attention module to generate correctly attributed instances at specified spatial positions. Second, to mitigate potential global semantic inconsistencies that may arise from IMCA, we propose a **Shared Timestep-Adaptive Prompt Enhancement (STAPE)** module, which connects local instances with global semantics and reduces artifact generation. Finally, to further improve the generation of small instances, we incorporate **Spatially-Aware Unconditional Guidance (SAUG)** during both training and inference, enhancing their fidelity and overall visual quality. For clarity, we omit all normalization layers and the batch dimension, and all indices are 1-indexed in the following description.

4.1. Instance-Aware Masked Cross-Attention

In the DiT backbone, the Cross-Attention module is responsible for cross-modal interactions and determining the semantics of generated videos [14, 27, 41], thus achieving fine-grained instance-level control necessitates imposing guidance upon this powerful mechanism.

Explicit Instance Prompt Injection. To maximize the influence of our instance-level information on cross-attention, the most efficient way is to inject the target visual tokens with semantic content that aligns with the context domain of following cross-attention module. Supposing that we obtain a set of N_v visual tokens, $\mathbf{V} = (V_1^1, V_2^1, \dots, V_{HW}^F)$, $V_i^t \in \mathbb{R}^D$ after VAE encoding and DiT patchification. The total number of tokens is $N_v = F \times H \times W$, corresponding to a latent feature map with temporal length F and spatial resolution $H \times W$. Previous methods for image-level instance control typically adopt CLIP-encoded features for instance representations, which are then fused with positional information through a neural network,

$$\bar{\mathbf{V}} = [\mathbf{V}, \text{MLP}(\text{Instance}_{\text{CLIP}}, \text{Position})] \quad (1)$$

The fused features are appended after visual tokens and incorporated into the backbone’s features via an added self-

attention module in a residual fashion,

$$\mathbf{V} = \mathbf{V} + \text{SelfAttn}(\overline{\mathbf{V}}, \overline{\mathbf{V}})[:\text{len}(\mathbf{V})] \quad (2)$$

However, this approach suffers from two key limitations, (1) the feature leakage issues inherent in CLIP embeddings [8] will be exacerbated in tasks involving longer video captions; (2) tasking a single neural network to simultaneously fuse positional information with instance features and align the resulting representation with backbone visual semantics introduces significant training complexity.

To fully leverage the backbone’s text encoding and cross-modal semantic alignment capabilities, we employ its native text encoder and text embedding layer to process the individual instance prompts to get instance prompt tokens $\mathbf{I} = \{\mathbf{I}^1, \mathbf{I}^2, \dots, \mathbf{I}^F\}$. Each set $\mathbf{I}^t = (I_1^t, I_2^t, \dots, I_{N_{ins}}^t)$, $I_i^t \in \mathbb{R}^{D_{ins}}$, contains up to N_{ins} tokens, with any shorter ones being zero-padded. Concurrently, we no longer encode positional information into \mathbf{I} , thereby avoiding any potential interference with their underlying semantics.

Instance-Aware Cross-Attention. Since visual tokens \mathbf{V} significantly outnumber instance prompt tokens \mathbf{I} , appending \mathbf{I} to \mathbf{V} and using a self-attention mechanism for information exchange is inefficient for instance-level injection. This inefficiency arises because visual tokens exhibit high self-similarity, causing them to dominate the attention mechanism. Furthermore, in video diffusion models, self-attention incurs substantially higher computational costs (in both FLOPS and time cost) compared to cross-attention. Therefore, we propose an Instance-Aware Cross-Attention module designed to reduce computational overhead while maximally integrating the semantics of instance prompt tokens into the visual tokens. This module is incorporated into the backbone via a residual connection [12] and is modulated by a zero-initialized gated parameter m_v to ensure training stability.

Attention Masks. To effectively inject explicit positional information, we employ attention masks $\mathbf{M} \in \mathbb{R}^{F \times N_{ins} \times N_v}$ that constrain each instance token to act only on its corresponding visual tokens. In modern deep learning frameworks, this implementation does not significantly increase the forward pass time, even in the absence of FlashAttention [6]. The attention mask \mathbf{M} is defined as follows:

$$M_{(i,j)}^t = \begin{cases} 1 & \text{if } [V_i^t, I_j^t] = 1, \\ -\text{inf} & \text{if } [V_i^t, I_j^t] = 0, \end{cases}$$

Here, $[V_i^t, I_j^t] = 1$ indicates that in frame- t , the visual token V_i^t and the instance prompt token I_j^t correspond to the same instance.

Better Initialization. The advantages of IMCA extend beyond explicit instance information injection and computational efficiency. A key benefit is that its weights can be initialized from the corresponding cross-attention module

within the same DiT Block. We find that this initialization strategy substantially reduces the model’s training time and enhances stability, particularly in the early stages, by providing more meaningful initial semantic guidance for the instance prompts.

Overall. Each DiT Block within the backbone is augmented with an IMCA module. Positioned between the self-attention and cross-attention blocks, this IMCA module operates as a residual branch modulated by a gated parameter m_v , to inject instance-specific information into the backbone’s visual tokens. As a result, when these semantically enhanced visual tokens are processed by the subsequent cross-attention module, they can achieve higher similarity with their corresponding segments in the video caption tokens.

$$\mathbf{V} = \mathbf{V} + \text{SelfAttn}(\mathbf{V}) \quad (3)$$

$$\mathbf{V} = \mathbf{V} + m_v \times \text{IMCA}(\mathbf{V}, \mathbf{I}, \mathbf{M}) \quad (4)$$

$$\mathbf{V} = \mathbf{V} + \text{CrossAttn}(\mathbf{V}, \mathbf{T}) \quad (5)$$

Since the overall semantic information of the video is injected entirely through the cross-attention module, this mechanism indirectly influences the cross-attention’s information injection, thereby enabling instance-level control.

4.2. Shared Timestep-Adaptive Prompt Enhancement Module

Since our instance prompt tokens are generated by encoding each instance prompt in isolation, they inherently lack global semantics. In contrast, the corresponding content within the global video caption $\mathbf{T} = (T_1, T_2, \dots, T_{N_{ctx}})$, $T_i \in \mathbb{R}^{D_{ctx}}$, contains richer contextual information, including inter-instance interactions and spatial relationships. Consequently, an identical set of instance prompts should yield entirely different outcomes depending on the overarching video caption.

Instance Prompts Enhancement. As previously discussed, the relationship between our IMCA module and the native Cross-Attention resembles an adversarial interplay. This challenge is compounded by our choice to freeze the backbone for training efficiency, which places the entire burden of this local-to-global semantic adjustment solely on the IMCA module. Furthermore, the instance-level information injected by IMCA is highly direct and forceful, which can lead to undesirable artifacts in the final output under certain circumstances. To address this issue, we propose the Instance Prompts Enhancement module, which is designed to inject global semantics into the separate instance prompts.

Timestep-Adaptive Modulation. The Instance Prompt Enhancement module is shared across all DiT blocks, analogous to the text encoder. However, since the contribution of each DiT block is not uniform across different dif-

Model	Resolution	General Metrics				Instance-aware metrics					
		FVD↓	Temporal↑	CLIP-B↑	CLIP-L↑	Area-Weighted Mean			Mean		
						IoU%↑	CLIP-B↑	CLIP-L↑	IoU%↑	CLIP-B↑	CLIP-L↑
Wan2.1	480P	2837.22	0.9834	0.3088	0.2480	0.2721	0.2172	0.1625	0.1454	0.2179	0.1635
Wan2.2	720P	2687.98	0.9867	0.3110	0.2495	0.2717	0.2207	0.1698	0.1547	0.2198	0.1720
HunyuanVideo	720P	2781.50	0.9808	0.2977	0.2395	0.3172	0.2178	0.1674	0.1543	0.2230	0.1700
CogVideoX	480P	3416.78	0.9939	0.3002	0.2483	0.2564	0.2138	0.1594	0.1339	0.2187	0.1635
SkyReelsV2	540P	3155.76	0.9797	0.2965	0.2461	0.2478	0.2154	0.1611	0.1386	0.2176	0.1631
InstanceV(ours)	480P	2313.06	0.9906	0.3123	0.2519	0.7298	0.2321	0.1793	0.6090	0.2322	0.1782
	720P	2285.22	0.9924	0.3167	0.2530	0.7228	0.2324	0.1838	0.5910	0.2313	0.1849

Table 2. Quantitative comparisons. We primarily report the results of the proposed InstanceV framework integrated with open-source state-of-the-art text-to-video diffusion models, evaluated at both 480P and 720P resolutions. The evaluation is conducted from two perspectives: (1) general video quality metrics, and (2) our proposed InstanceBench for instance-level assessment.

fusion timesteps, a static enhancement would be suboptimal. To ensure the module’s contribution is both adaptive and timestep-aware, we implement the residual gated parameter m_t as a D_{ins} -dimensional tensor, enabling a more fine-grained, adaptive modification. Crucially, to achieve this temporal awareness in a parameter-efficient manner, we compute α_1 by repurposing one of the six adaptive modulation parameters from the DiT block’s native AdaLN layer [29],

$$\mathbf{I} = \mathbf{I} + (m_t + \alpha_1) \times \text{CrossAttn}(\mathbf{I}, \mathbf{T}) \quad (6)$$

4.3. Spatially-Aware Unconditional Guidance

Due to the limitations of bounding boxes, certain visual tokens may correspond to more than one instance token. After further patchification through the VAE and DiT backbone, some instances may correspond to only a small number of visual tokens. This can easily lead to the disappearance of small instances that overlap with larger ones. To address this issue, we further propose a variation of classifier-free-guidance [16], termed Spatially-Aware Unconditional Guidance.

During the unconditional forward pass, the attention masks are still applied to inject explicit spatial information, while the corresponding instance prompts are left empty,

$$\tilde{\epsilon}_\theta(\mathbf{z}, \mathbf{I}, \mathbf{M}) = (1 + w)\epsilon_\theta(\mathbf{z}, \mathbf{I}, \mathbf{M}) - w\epsilon_\theta(\mathbf{z}, \mathbf{M}). \quad (7)$$

This setup allows the cross-attention module to receive positional cues while leaving semantic content unset. As a result, the cross-attention module can better reason about hierarchical relationships among different instances from a global perspective, reducing the overly flattened semantic interference from large instances and thereby improving the generation of smaller instances. In implementation, for the empty instance prompts, we reuse the $\langle \text{extra_id} \rangle$ tokens from the text encoder. Compared with introducing new tokens, the pretrained $\langle \text{extra_id} \rangle$ tokens naturally possess richer and more general semantic representations.

5. Experiments

5.1. Implementation Details

5.1.1. Baselines

We compare our model against state-of-the-art methods, including Wan, HunyuanVideo, CogVideoX, and SkyReelsV2. Since InstanceCap has not released any fine-tuned models, we implement a substitute version as described in the supplementary material. Following Figure. 1, we generate a total of 100 videos for each model in 5 groups, including (1) main subjects, (2) dense small objects, (3) complex scene settings, (4) trajectory control, and (5) camera control.

5.2. Evaluation Metrics

and VBench2, We design a comprehensive InstanceBench for instance-aware evaluation of video diffusion models. InstanceBench consists of two sets of metrics. For general-purpose evaluation, we include FVD [35], Temporal [21], and CLIPScore metrics. For instance-aware evaluation, we design two complementary testing protocols, supposing that a set of instance information is obtained using the pipeline described in Section 3 for both real and generated videos, (1) For instances sharing the same label, we compute the bounding box IoU [33] to measure spatial alignment and layout consistency. (2) We extract from generated videos the image patches within the ground-truth bounding boxes and compute their CLIP-Score with the corresponding instance prompts to evaluate visual-semantic fidelity. Together, these two protocols provide a joint evaluation of layout accuracy and instance-level visual quality. However, simply averaging the IoU and CLIP-Score across instances of different sizes can be unfair due to their varying degrees of influence on the generated video. To address this, we additionally evaluate area-weighted IoU and area-weighted CLIP-Score, which better reflect the semantic and visual contributions of different instances.

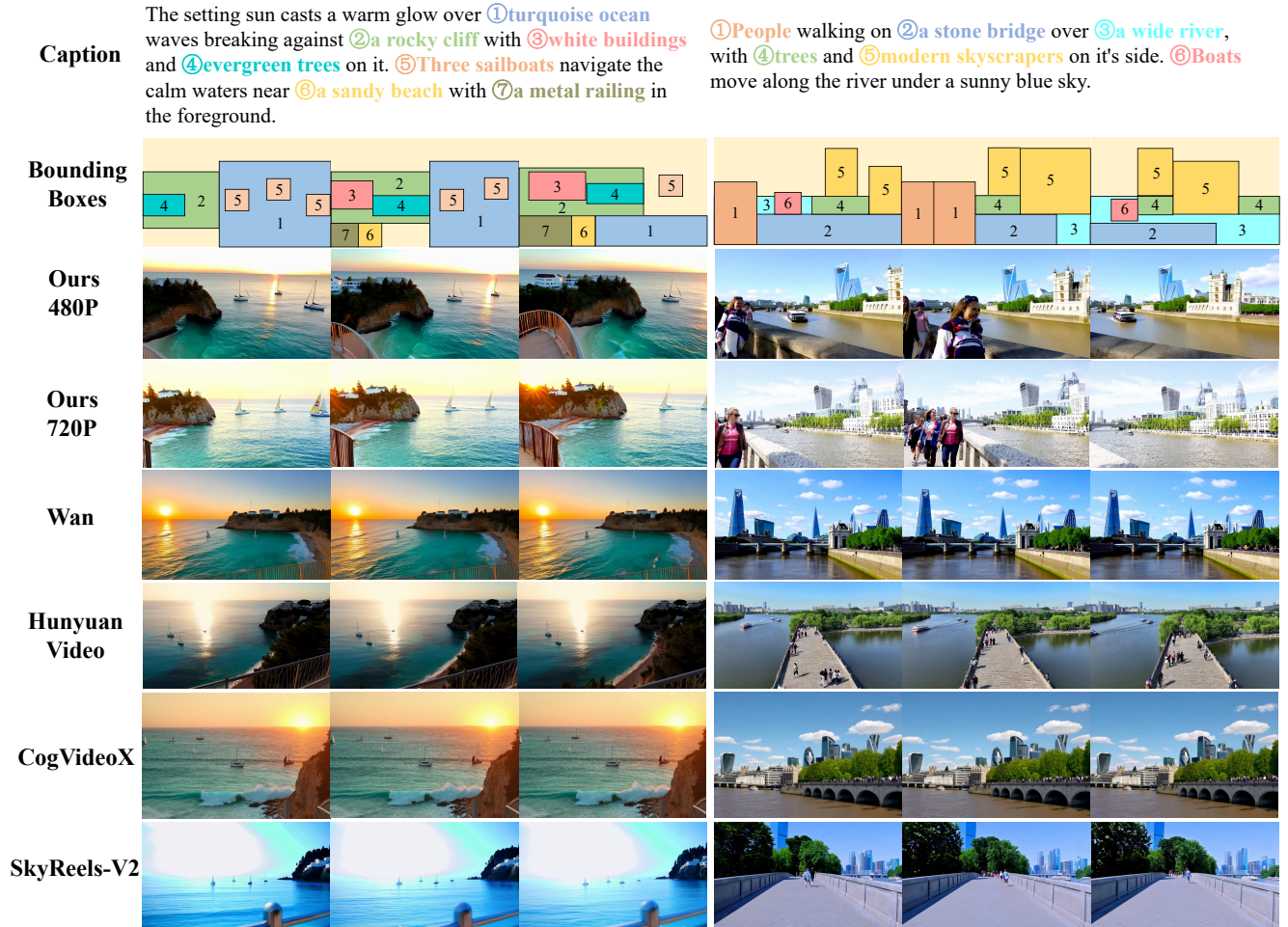


Figure 3. Quality comparison between our proposed InstanceV and state-of-the-art video diffusion models. The first, middle, and last frames are shown for illustration.

5.3. Comparison Results

5.3.1. Qualitative comparisons

As show in Figure, InstanceV achieves accurate instance-level control conditioned on the additional grounding information. While maintaining the overall visual quality of the backbone, it further enhances the fidelity of instance-specific details. Moreover, both inter-instance relations and the consistency between local instances and global semantics are well preserved. In addition, control conditions that are difficult to express purely through text, such as camera motion, can also be indirectly achieved via instance-level grounding information. Without additional instance-level grounding information, different models tend to produce visually diverse videos even when conditioned on the same caption. We observe that existing state-of-the-art models often fail to accurately represent instance-level semantics, trapping themselves in missing or misattributed instances even explicitly described in the caption. More-

over, although the captions may clearly describe motion, the corresponding instances are sometimes generated too small or too blurred, resulting in videos that appear overly static. Specifically, outputs from the Wan-series and HunyuanVideo models may contain noticeable artifacts under more complex semantics. While HunyuanVideo produces videos with richer motion dynamics, this often comes at the expense of temporal consistency. In contrast, CogVideoX frequently generates nearly static videos, lacking sufficient motion cues and resulting in visually stagnant scenes. For SkyReelV2, videos with moderately complex motion often exhibit frame-to-frame flickering and suffer from poor temporal coherence.

5.3.2. Quantitative Comparisons

From the quantitative results, our InstanceV framework shows a notable improvement in FVD, indicating a significant enhancement in faithfully restoring the visual semantics expressed by the prompts. Meanwhile, the text-

(a) Ablation on Instance-aware Masked Cross Attention

ⓐ Artificial Christmas trees stand on a ⓑ wooden staircase with ⓓ red carpeting; ⓔ two classical paintings of children wearing green dresses hang on the wall while ⓖ several people walk through an ⓗ open doorway.



(c) Ablation on Spatially-Aware Unconditional Guidance

ⓐ A snail with ⓑ a pinkish-brown spiral shell and ⓓ two white tentacles, with ⓔ a bright red ladybug resting on its shell, is positioned on ⓖ a bed of bright green moss.



(b) Ablation on Shared Timestep-Adaptive Prompt Enhancement Module

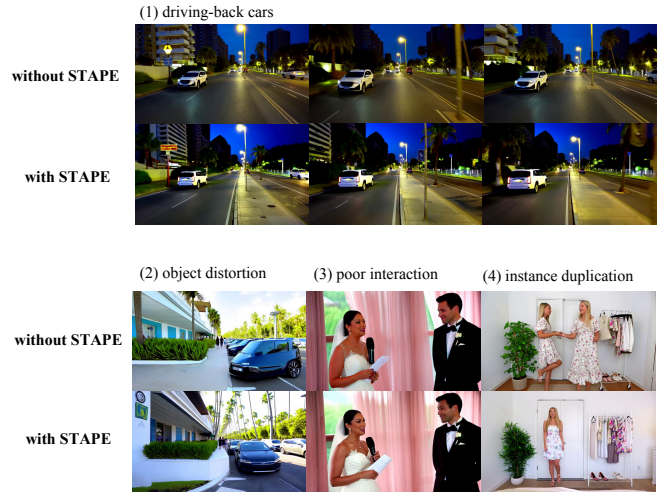


Figure 4. Ablation studies on the proposed modules.

Backbone	IMCA	STAPE	SAUG	Temporal	Area-Weighted Mean		
					IoU% \uparrow	CLIP-B% \uparrow	CLIP-L% \uparrow
✓				0.9834	0.2721	0.2172	0.1625
✓	✓			0.9885	0.7157	0.2315	0.1781
✓	✓	✓		0.9903	0.7082	0.2303	0.1766
✓	✓	✓	✓	0.9906	0.7298	0.2321	0.1793

Table 3. Quantitative Ablation Studies.

to-video alignment also improves, suggesting that incorporating instance-level grounding information helps the model generate videos that more accurately correspond to the intended textual semantics. Although InstanceV shows slightly lower scores in temporal consistency compared to CogVideoX, we observe that this is mainly because CogVideoX tends to generate overly static videos with limited motion. Our proposed InstanceV framework also demonstrates significant improvements when it comes to instance-aware metrics. From the IoU metric, it is evident that incorporating additional instance-level grounding information substantially enhances the layout quality of the generated videos. This improvement becomes even more pronounced when evaluated using the area-weighted IoU, which better reflects the influence of larger instances on the overall visual structure. Although the 480P version of InstanceV achieves slightly higher IoU scores than the 720P version, the 720P version outperforms in terms of CLIP-Score, benefiting from its higher resolution.

5.4. Ablation Studies

We conduct ablation studies on three variants: (1) Instance-aware Masked Cross-Attention (2) Shared Timestep-Adaptive Prompt Enhancement Module (3) Spatially-Aware Unconditional Guidance. As shown in Fig. 4(a), the Instance-aware Masked Cross-Attention module plays a

crucial role in determining the overall video layout and motion range. Under complex semantics, it helps the model better understand the feature attributes and spatial positions of different instances described in the overall video caption. This mechanism further enables more reasonable interactions and associations among instances, thereby alleviating artifacts and preventing the generation of completely static videos. Due to the limited influence of mutually independent instance prompts on the overall semantics, various types of artifacts occur, as shown in Fig. 4(b), including: (1) semantic errors caused by reversed motions of vehicles or humans; (2) visual semantic distortions due to malformed instance appearances; (3) disconnection artifacts, where interactions between different instances are lost; (4) duplicated instances caused by disagreements between IMCA and native cross-attention. With the help of STAPE, these issues are effectively alleviated, leading to improved overall temporal consistency and text-visual alignment, as shown in Table 3. Benefiting from proposed SAUG, the generation of small objects is significantly improved. We observe increases in IoU and CLIPScore as shown in Table. 3, indicating that these small objects are no longer overlooked and can meaningfully contribute to the overall semantic of the generated video.

6. Conclusion

In this work, we propose InstanceV, a novel framework for instance-level controllable video generation. By leveraging Instance-aware Masked Cross-Attention mechanism, InstanceV is able to generate instances with precise spatial localization and well-defined attributes. The proposed Shared Timestep-Adaptive Prompt Enhancement Module improves the coherence between local instance semantics and global

video context in a parameter-efficient manner. In addition, a Spatially-Aware Unconditional Guidance strategy is incorporated during both training and inference to further refine the details and fidelity of small instances. Extensive experiments demonstrate that InstanceV achieves not only accurate instance-level control, but also stronger alignment with video captions and richer instance details, jointly contributing to a significant improvement in the overall quality of generated videos.

References

- [1] Sherwin Bahmani, Ivan Skorokhodov, Aliaksandr Siarohin, Willi Menapace, Guocheng Qian, Michael Vasilkovsky, Hsin-Ying Lee, Chaoyang Wang, Jiayu Zou, Andrea Tagliasacchi, et al. Vd3d: Taming large video diffusion transformers for 3d camera control. *arXiv preprint arXiv:2407.12781*, 2024. 3
- [2] Joao Carreira and Andrew Zisserman. Quo vadis, action recognition? a new model and the kinetics dataset. In *proceedings of the IEEE Conference on Computer Vision and Pattern Recognition*, pages 6299–6308, 2017. 11
- [3] Di Chang, Yichun Shi, Quankai Gao, Jessica Fu, Hongyi Xu, Guoxian Song, Qing Yan, Yizhe Zhu, Xiao Yang, and Mohammad Soleymani. Magicpose: Realistic human poses and facial expressions retargeting with identity-aware diffusion. *arXiv preprint arXiv:2311.12052*, 2023. 3
- [4] Guibin Chen, Dixuan Lin, Jiangping Yang, Chunze Lin, Junchen Zhu, Mingyuan Fan, Hao Zhang, Sheng Chen, Zheng Chen, Chengcheng Ma, et al. Skyreels-v2: Infinite-length film generative model. *arXiv preprint arXiv:2504.13074*, 2025. 2, 12
- [5] Jiahao Cui, Hui Li, Yao Yao, Hao Zhu, Hanlin Shang, Kaihui Cheng, Hang Zhou, Siyu Zhu, and Jingdong Wang. Hallo2: Long-duration and high-resolution audio-driven portrait image animation. *arXiv preprint arXiv:2410.07718*, 2024. 3
- [6] Tri Dao, Dan Fu, Stefano Ermon, Atri Rudra, and Christopher Ré. FlashAttention: Fast and memory-efficient exact attention with IO-awareness. In *Advances in Neural Information Processing Systems*, pages 16344–16359, 2022. 5
- [7] Tiejun Fan, Kepan Nan, Rui Xie, Penghao Zhou, Zhenheng Yang, Chaoyou Fu, Xiang Li, Jian Yang, and Ying Tai. InstanceCap: Improving Text-to-Video Generation via Instance-aware Structured Caption. In *Proceedings of the IEEE/CVF Conference on Computer Vision and Pattern Recognition*, pages 28974–28983, 2025. 3, 12
- [8] Weixi Feng, Xuehai He, Tsu-Jui Fu, Varun Jampani, Arjun Akula, Pradyumna Narayana, Sugato Basu, Xin Eric Wang, and William Yang Wang. Training-free structured diffusion guidance for compositional text-to-image synthesis. *arXiv preprint arXiv:2212.05032*, 2022. 5
- [9] Yossi Gandelsman, Alexei A Efros, and Jacob Steinhardt. Interpreting clip’s image representation via text-based decomposition. *arXiv preprint arXiv:2310.05916*, 2023. 16
- [10] Xavier Glorot and Yoshua Bengio. Understanding the difficulty of training deep feedforward neural networks. In *Proceedings of the thirteenth international conference on artificial intelligence and statistics*, pages 249–256. JMLR Workshop and Conference Proceedings, 2010. 16
- [11] Zekai Gu, Rui Yan, Jiahao Lu, Peng Li, Zhiyang Dou, Chenyang Si, Zhen Dong, Qifeng Liu, Cheng Lin, Ziwei Liu, Wenping Wang, and Yuan Liu. Diffusion as Shader: 3D-aware Video Diffusion for Versatile Video Generation Control. In *Proceedings of the Special Interest Group on Computer Graphics and Interactive Techniques Conference Conference Papers*, pages 1–12, 2025. 3
- [12] Kaiming He, Xiangyu Zhang, Shaoqing Ren, and Jian Sun. Deep residual learning for image recognition. In *Proceedings of the IEEE Conference on Computer Vision and Pattern Recognition (CVPR)*, pages 770–778, 2016. 5
- [13] Xuan He, Dongfu Jiang, Ge Zhang, Max Ku, Achint Soni, Sherman Siu, Haonan Chen, Abhramil Chandra, Ziyang Jiang, Aaran Arulraj, et al. Videoscore: Building automatic metrics to simulate fine-grained human feedback for video generation. In *Proceedings of the 2024 Conference on Empirical Methods in Natural Language Processing*, pages 2105–2123, 2024. 13
- [14] Amir Hertz, Ron Mokady, Jay Tenenbaum, Kfir Aberman, Yael Pritch, and Daniel Cohen-Or. Prompt-to-prompt image editing with cross attention control. *arXiv preprint arXiv:2208.01626*, 2022. 4
- [15] Jack Hessel, Ari Holtzman, Maxwell Forbes, Ronan Le Bras, and Yejin Choi. Clipscore: A reference-free evaluation metric for image captioning. In *Proceedings of the 2021 conference on empirical methods in natural language processing*, pages 7514–7528, 2021. 11
- [16] Jonathan Ho and Tim Salimans. Classifier-free diffusion guidance. *arXiv preprint arXiv:2207.12598*, 2022. 6, 12
- [17] Teng Hu, Zhentao Yu, Zhengguang Zhou, Sen Liang, Yuan Zhou, Qin Lin, and Qinglin Lu. Hunyuancustom: A multimodal-driven architecture for customized video generation. *arXiv preprint arXiv:2505.04512*, 2025. 2
- [18] Teng Hu, Zhentao Yu, Zhengguang Zhou, Jiangning Zhang, Yuan Zhou, Qinglin Lu, and Ran Yi. Polyvivid: Vivid multi-subject video generation with cross-modal interaction and enhancement. *arXiv preprint arXiv:2506.07848*, 2025. 3
- [19] Teng Hu, Jiangning Zhang, Zihan Su, and Ran Yi. Ultragen: High-resolution video generation with hierarchical attention. *arXiv preprint arXiv:2510.18775*, 2025. 2
- [20] Chi-Pin Huang, Yen-Siang Wu, Hung-Kai Chung, Kai-Po Chang, Fu-En Yang, and Yu-Chiang Frank Wang. Videoimage: Multi-subject and motion customization of text-to-video diffusion models. In *Proceedings of the Computer Vision and Pattern Recognition Conference*, pages 17603–17612, 2025. 2
- [21] Ziqi Huang, Yanan He, Jiashuo Yu, Fan Zhang, Chenyang Si, Yuming Jiang, Yuanhan Zhang, Tianxing Wu, Qingyang Jin, Nattapol Chanpaisit, Yaohui Wang, Xinyuan Chen, Limin Wang, Dahua Lin, Yu Qiao, and Ziwei Liu. VBench: Comprehensive benchmark suite for video generative models. In *CVPR*, pages 21807–21818, 2024. 6, 11, 13
- [22] Ziqi Huang, Fan Zhang, Xiaojie Xu, Yanan He, Jiashuo Yu, Ziyue Dong, Qianli Ma, Nattapol Chanpaisit, Chenyang Si, Yuming Jiang, et al. Vbench++: Comprehensive and ver-

- satellite benchmark suite for video generative models. *arXiv preprint arXiv:2411.13503*, 2024. 14
- [23] Zeyinzi Jiang, Zhen Han, Chaojie Mao, Jingfeng Zhang, Yulin Pan, and Yu Liu. Vace: All-in-one video creation and editing. In *Proceedings of the IEEE/CVF International Conference on Computer Vision*, pages 17191–17202, 2025. 3
- [24] Weijie Kong, Qi Tian, Zijian Zhang, Rox Min, Zuozhuo Dai, Jin Zhou, Jiangfeng Xiong, Xin Li, Bo Wu, Jianwei Zhang, et al. Hunyuanvideo: A systematic framework for large video generative models. *arXiv preprint arXiv:2412.03603*, 2024. 2, 12
- [25] Yuheng Li, Haotian Liu, Qingyang Wu, Fangzhou Mu, Jianwei Yang, Jianfeng Gao, Chunyuan Li, and Yong Jae Lee. GLIGEN: Open-set grounded text-to-image generation. In *2023 IEEE/CVF Conference on Computer Vision and Pattern Recognition (CVPR)*, pages 22511–22521, 2023. 2, 3, 16
- [26] Haokun Lin, Haoli Bai, Zhili Liu, Lu Hou, Muye Sun, Linqi Song, Ying Wei, and Zhenan Sun. Mope-clip: Structured pruning for efficient vision-language models with module-wise pruning error metric. In *Proceedings of the IEEE/CVF conference on computer vision and pattern recognition*, pages 27370–27380, 2024. 16
- [27] Shaoteng Liu, Yuechen Zhang, Wenbo Li, Zhe Lin, and Jiaya Jia. Video-p2p: Video editing with cross-attention control. In *Proceedings of the IEEE/CVF Conference on Computer Vision and Pattern Recognition*, pages 8599–8608, 2024. 4
- [28] Rang Meng, Xingyu Zhang, Yuming Li, and Chenguang Ma. EchoMimicV2: Towards Striking, Simplified, and Semi-Body Human Animation. In *Proceedings of the IEEE/CVF Conference on Computer Vision and Pattern Recognition*, pages 5489–5498, 2025. 3
- [29] William Peebles and Saining Xie. Scalable diffusion models with transformers. In *ICCV*, pages 4195–4205, 2023. 2, 6
- [30] Alec Radford, Jong Wook Kim, Chris Hallacy, A. Ramesh, Gabriel Goh, Sandhini Agarwal, Girish Sastry, Amanda Askell, Pamela Mishkin, Jack Clark, Gretchen Krueger, and I. Sutskever. Learning Transferable Visual Models From Natural Language Supervision. In *International Conference on Machine Learning*, 2021. 3, 11
- [31] Nikhila Ravi, Valentin Gabeur, Yuan-Ting Hu, Ronghang Hu, Chaitanya Ryali, Tengyu Ma, Haitham Khedr, Roman Rädle, Chloe Rolland, Laura Gustafson, et al. Sam 2: Segment anything in images and videos. *arXiv preprint arXiv:2408.00714*, 2024. 3
- [32] Tianhe Ren, Shilong Liu, Ailing Zeng, Jing Lin, Kunchang Li, He Cao, Jiayu Chen, Xinyu Huang, Yukang Chen, Feng Yan, et al. Grounded sam: Assembling open-world models for diverse visual tasks. *arXiv preprint arXiv:2401.14159*, 2024. 3
- [33] Hamid Rezaatofghi, Nathan Tsoi, JunYoung Gwak, Amir Sadeghian, Ian Reid, and Silvio Savarese. Generalized intersection over union: A metric and a loss for bounding box regression. *arXiv preprint arXiv:1902.09630*, 2019. 6, 11
- [34] Etai Sella, Yanir Kleiman, and Hadar Averbuch-Elor. Instancegen: Image generation with instance-level instructions. In *Proceedings of the Special Interest Group on Computer Graphics and Interactive Techniques Conference Conference Papers*, pages 1–10, 2025. 2, 3, 11
- [35] Thomas Unterthiner, Sjoerd Van Steenkiste, Karol Kurach, Raphael Marinier, Marcin Michalski, and Sylvain Gelly. Towards accurate generative models of video: A new metric & challenges. *arXiv preprint arXiv:1812.01717*, 2018. 6
- [36] Thomas Unterthiner, Sjoerd Van Steenkiste, Karol Kurach, Raphaël Marinier, Marcin Michalski, and Sylvain Gelly. Fvd: A new metric for video generation. 2019. 11
- [37] Ashish Vaswani, Noam Shazeer, Niki Parmar, Jakob Uszkoreit, Llion Jones, Aidan N Gomez, Lukasz Kaiser, and Illia Polosukhin. Attention is all you need. *Advances in neural information processing systems*, 30, 2017. 16
- [38] Team Wan, Ang Wang, Baole Ai, Bin Wen, Chaojie Mao, Chen-Wei Xie, Di Chen, Feiwu Yu, Haiming Zhao, Jianxiao Yang, et al. Wan: Open and advanced large-scale video generative models. *arXiv preprint arXiv:2503.20314*, 2025. 2, 12
- [39] Mengchao Wang, Qiang Wang, Fan Jiang, Yaqi Fan, Yunpeng Zhang, Yonggang Qi, Kun Zhao, and Mu Xu. Fantasytalking: Realistic talking portrait generation via coherent motion synthesis. *arXiv preprint arXiv:2504.04842*, 2025. 3
- [40] Xudong Wang, Trevor Darrell, Sai Saketh Rambhatla, Rohit Girdhar, and Ishan Misra. InstanceDiffusion: Instance-level control for image generation. In *CVPR*, pages 6232–6242, 2024. 2, 3, 11, 16
- [41] Yuxin Wen, Jim Wu, Ajay Jain, Tom Goldstein, and Ashwin Panda. Analysis of attention in video diffusion transformers. *arXiv preprint arXiv:2504.10317*, 2025. 4
- [42] Haocheng Xi, Shuo Yang, Yilong Zhao, Chenfeng Xu, Muyang Li, Xiuyu Li, Yujun Lin, Han Cai, Jintao Zhang, Dacheng Li, et al. Sparse videogen: Accelerating video diffusion transformers with spatial-temporal sparsity. *arXiv preprint arXiv:2502.01776*, 2025. 17
- [43] Bin Xiao, Haiping Wu, Weijian Xu, Xiyang Dai, Houdong Hu, Yumao Lu, Michael Zeng, Ce Liu, and Lu Yuan. Florence-2: Advancing a Unified Representation for a Variety of Vision Tasks. In *Proceedings of the IEEE/CVF Conference on Computer Vision and Pattern Recognition*, pages 4818–4829, 2024. 3
- [44] Jinbo Xing, Long Mai, Cusuh Ham, Jiahui Huang, Anirudha Mahapatra, Chi-Wing Fu, Tien-Tsin Wong, and Feng Liu. MotionCanvas: Cinematic Shot Design with Controllable Image-to-Video Generation. In *Proceedings of the Special Interest Group on Computer Graphics and Interactive Techniques Conference Conference Papers*, pages 1–11, 2025. 3
- [45] Linting Xue, Noah Constant, Adam Roberts, Mihir Kale, Rami Al-Rfou, Aditya Siddhant, Aditya Barua, and Colin Raffel. mt5: A massively multilingual pre-trained text-to-text transformer. In *Proceedings of the 2021 conference of the North American chapter of the association for computational linguistics: Human language technologies*, pages 483–498, 2021. 16
- [46] An Yang, Beichen Zhang, Binyuan Hui, Bofei Gao, Bowen Yu, Chengpeng Li, Dayiheng Liu, Jianhong Tu, Jingren Zhou, Junyang Lin, et al. Qwen2.5 technical report. *arXiv preprint arXiv:2412.15115*, 2024. 3

- [47] Zhuoyi Yang, Jiayan Teng, Wendi Zheng, Ming Ding, Shiyu Huang, Jiazheng Xu, Yuanming Yang, Wenyi Hong, Xiaohan Zhang, Guanyu Feng, et al. Cogvideox: Text-to-video diffusion models with an expert transformer. *arXiv preprint arXiv:2408.06072*, 2024. 2, 12
- [48] Shenghai Yuan, Jinfa Huang, Xianyi He, Yunyang Ge, Yujun Shi, Liuhan Chen, Jiebo Luo, and Li Yuan. Identity-Preserving Text-to-Video Generation by Frequency Decomposition. In *Proceedings of the IEEE/CVF Conference on Computer Vision and Pattern Recognition*, pages 12978–12988, 2025. 3
- [49] Zhihang Yuan, Hanling Zhang, Lu Pu, Xuefei Ning, Linfeng Zhang, Tianchen Zhao, Shengen Yan, Guohao Dai, and Yu Wang. Ditfastatt: Attention compression for diffusion transformer models. *Advances in Neural Information Processing Systems*, 37:1196–1219, 2024. 17
- [50] Zhenghao Zhang, Junchao Liao, Menghao Li, ZuoZhuo Dai, Bingxue Qiu, Siyu Zhu, Long Qin, and Weizhi Wang. Tora: Trajectory-oriented Diffusion Transformer for Video Generation. In *CVPR*, pages 2063–2073, 2025. 3
- [51] Dian Zheng, Ziqi Huang, Hongbo Liu, Kai Zou, Yanan He, Fan Zhang, Lulu Gu, Yuanhan Zhang, Jingwen He, Wei-Shi Zheng, et al. Vbench-2.0: Advancing video generation benchmark suite for intrinsic faithfulness. *arXiv preprint arXiv:2503.21755*, 2025. 14
- [52] Guangcong Zheng, Xianpan Zhou, Xuewei Li, Zhongang Qi, Ying Shan, and Xi Li. LayoutDiffusion: Controllable diffusion model for layout-to-image generation. In *CVPR*, pages 22490–22499, 2023. 2, 3
- [53] Zangwei Zheng, Xiangyu Peng, Tianji Yang, Chenhui Shen, Shenggui Li, Hongxin Liu, Yukun Zhou, Tianyi Li, and Yang You. Open-sora: Democratizing efficient video production for all. *arXiv preprint arXiv:2412.20404*, 2024. 2, 12
- [54] Dewei Zhou, You Li, Fan Ma, Xiaoting Zhang, and Yi Yang. MIGC: Multi-instance generation controller for text-to-image synthesis. In *CVPR*, pages 6818–6828, 2024. 2, 3

7. Overview

The supplementary material is composed of:

- Computational efficiency analysis (Sec. 8)
- Implementation details and more comparison results. (Sec. 9)
- More details and discussion on model implementation (Sec. 10)
- Potential limitations and future work (Sec. 10)

8. Computational Efficiency Analysis

As shown in Table.1 in main text, our proposed instance-level control framework **InstanceV** achieves *significantly lower parameter overhead* and *higher computational efficiency* compared to previous approaches. It is worth noting that InstanceGen [34] *has not released* its official implementation, and thus the results reported for InstanceGen in Table.1 of the main text are based on our theoretical analysis.

More Comparison Details: (1) The reported added parameters are measured relative to the video diffusion model backbone,

which may include not only DiT blocks but also additional components such as timestep embedding layers, text embedding layers, and patchifying modules for video tokenization, depending on the specific implementation. (2) The added time cost is computed as the *average extra* inference time required to generate **100** samples, grounded additionally by **5** instance-level annotations. We constrain the number of instances because, for some existing approaches [40], the instance count can directly affect the required number of *denoising steps*, which would otherwise lead to unfair comparisons.

We provide the FLOPs of each component within a single DiT block for generating a 480P video. Note that the added FLOPs reported in Table.1 of the main text correspond to the entire VDM backbone. Therefore, the FLOPs estimated from the table below may slightly differ from the results reported in Table.1 of the main text due to implementation variations and additional architectural components.

9. Implementation Details

9.1. Metrics

General Metrics.

- **FVD** Fréchet Video Distance (FVD) [36] is a widely adopted metric for evaluating the quality of generated videos. Similar to the Fréchet Inception Distance (FID) used in image generation, FVD measures the distributional distance between real and generated video feature representations extracted by a pretrained spatiotemporal network (typically an I3D model [2]). It jointly accounts for both visual fidelity and temporal consistency by capturing correlations across consecutive frames. Lower FVD values indicate that the generated videos are closer to real ones in terms of appearance and motion dynamics, and thus represent better overall generation quality.
- **Temporal** In the VBench [21] benchmark suite, one of the key dimensions under Temporal Quality is *Motion Smoothness*. Rather than measuring an abstract “temporal score,” VBench quantifies how physically plausible and fluid the motion in generated videos is: it compares the actual frames with interpolated frames (via a frame-interpolation model) and computes discrepancies to reflect coherence and naturalness of motion. A higher motion smoothness score indicates that the generated video exhibits more stable and realistic motion over time, with fewer sudden jitters or unnatural transitions.
- **CLIP-Score** CLIP Score [15] leverages the pretrained CLIP model [30] to evaluate the semantic alignment between generated visual content and the corresponding text descriptions. Specifically, both the image and its associated prompt are encoded into a shared multimodal embedding space, and their similarity is measured using cosine similarity. A higher CLIP Score indicates stronger semantic consistency between the visual appearance and the textual intent. Since CLIP is trained on a large corpus of diverse image–text pairs, this metric provides a robust and scalable evaluation of high-level semantic relevance in generative tasks. *For videos, we compute the CLIP score for each individual frame and then take the average across all frames to obtain a video-level CLIP score.*

Instance-aware Metrics

- IoU Intersection over Union (IoU) [33], also known as the Jac-

Methods	Resolution	Visual Quality \uparrow	Temporal Consistency \uparrow	Dynamic Degree \uparrow	Text-to-Video Alignment \uparrow	Factual Consistency \uparrow
Wan2.1 [38]	480P	2.99355	3.14705	3.22359	3.40019	2.96861
Wan2.2	720P	2.93241	3.11781	3.00619	3.25030	2.96679
HunyuanVideo [24]	720P	2.84249	3.02305	2.89554	3.14622	2.88761
CogVideoX [47]	480P	2.61276	2.79843	2.84793	3.05415	2.62031
SkyReelsV2 [4]	540P	2.62439	2.81272	2.76471	3.05063	2.63757
InstanceV(ours)	480P	3.10872	3.16971	3.42722	3.47803	3.05342
	720P	3.03335	3.23439	3.20825	3.33263	3.11876

Table 4. Quantitative comparison of our proposed InstanceV with state-of-the-art video diffusion models using *VideoScore*.

Methods	Resolution	Visual Quality \uparrow	Temporal Consistency \uparrow	Dynamic Degree \uparrow	Text-to-Video Alignment \uparrow	Factual Consistency \uparrow
Wan2.1	480P	2.98814	2.87894	3.15407	3.19866	2.79638
Wan2.2	720P	3.22745	3.20388	3.12385	3.14581	3.18957
HunyuanVideo	720P	2.99697	2.99133	2.88472	2.91647	2.99167
CogVideoX	480P	2.67665	2.69979	2.71733	2.78533	2.61382
SkyReelsV2	540P	2.63698	2.68429	2.59490	2.75576	2.59753
InstanceV(ours)	480P	3.33516	3.24925	3.52941	3.43886	3.22753
	720P	3.49686	3.44247	3.49406	3.35064	3.45481

Table 5. Quantitative comparison of our proposed InstanceV with state-of-the-art video diffusion models using *VideoScore-V1.1*.

card Index, is a widely used metric for evaluating the overlap between two sets, commonly applied in object detection and segmentation tasks. Given a predicted region A and a ground-truth region B , the IoU is defined as the ratio of the area of their intersection to the area of their union:

$$\text{IoU}(A, B) = \frac{|A \cap B|}{|A \cup B|} = \frac{|A \cap B|}{|A| + |B| - |A \cap B|}.$$

IoU values range from 0 to 1, where 0 indicates no overlap and 1 indicates perfect alignment. In video or instance-level tasks, IoU can be computed per frame or per instance, and averaged to assess temporal or multi-object consistency. The CLIP-B and CLIP-L metrics reported in Table.2 and Table.3 of the main text are computed using the CLIP-ViT-B/32 and CLIP-ViT-L/14 models, respectively. The definition of IoU in the instance-aware metrics is consistent with the above; *if a specific instance does not appear in the generated video, its IoU is assigned a value of 0.*

- Instance-level CLIP-Score The instance-level CLIP-Score is computed in the same manner as the standard CLIP-Score. Specifically, each instance is first cropped from the image according to its bounding box and then resized to the required input size before computing the CLIP-Score. *If a particular instance does not appear in the generated video, its CLIP-Score is set to 0.*

9.2. Experiment settings.

Training Details. During training, we adopt a batch size of 2 and use the Adam optimizer with bfloat16 precision. For the proposed SAUG strategy, we adopt an unconditional forward pass probability of 20% during training, following the standard practice in classifier-free guidance [16]. We observed that due to the limited numerical precision of bfloat16, the learning rate, as well as the magnitude of certain added-parameter layers and their gradients, some parameters occasionally ceased updating after reaching specific values. To address this issue, we employ a staged learning

rate schedule: **(1)** for the first 1,000 steps, a learning rate of 1e-5 is used to ensure stability at the early stage of training; **(2)** from step 1,000 to 3,000, the learning rate is linearly increased to 5e-4; **(3)** the learning rate is maintained at 5e-4 until step 8,000; **(4)** finally, it is linearly decreased back to 1e-5 until step 10,000 to guarantee stable convergence in the later stages of training.

Testing Details.

CFG. During inference, *we set the CFG scale to 5*, which is identical to the setting used for the backbone’s general text-to-video generation task. For the added modules, *all additional instance-level grounding inputs are replaced with all-zero tensors during unconditional forward passes.* The influence of different CFG scales on the final generated videos is illustrated in Figure. 5. Since the backbone uses a CFG scale of 5 for its original text-to-video task during inference, *setting the CFG scale below 5 leads to two issues: (1)* the additional instance-level grounding information has only a minimal effect, and *(2)* the text–visual alignment becomes noticeably weaker. When the CFG scale is increased beyond 5, we observe that although the model can, in some cases, better follow the instance-level grounding inputs, the overall visual quality of the generated videos slightly degrades. For example, the contrast becomes overly high and certain colors are lost, which noticeably reduces the distinguishability between similar hues and causes the boundaries between different instances to appear blurred. Considering this trade-off, we therefore adopt a CFG scale of 5 as our default setting.

9.3. More comparisons

InstanceCap InstanceCap [7] is the first work to introduce the concept of instance-level video generation, *but it does not address this problem at the model-architecture level.* Instead, it proposes an instance-level captioner and constructs instance-level training data, which are then used to finetune existing open-source video generation models, like Open-Sora [53]. Since the finetuned model weights of InstanceCap are not publicly available,



Figure 5. Ablation on CFG scale. We compare three settings (CFG = 5, 6, 7) by visualizing four representative videos, each shown with its first frame, a middle frame, and the final frame.

our comparison is conducted using the combination described in the original paper, namely the InstanceCap captioner with the original Open-Sora model. Concretely, we first process a given caption using the instance-level captioner, and then directly feed the resulting instance-aware caption into Open-Sora for video generation.

We evaluate the performance of InstanceCap on the same test cases used in Figure.3 of the main text. Due to GPU limitations, we generate only the 256-px version of each video. The left side of Figure. 6 shows the outputs of InstanceCap. Given a text prompt and an input video, InstanceCap produces instance-level video captions. For brevity, we omit the original video frames. As shown, the instance-captioner generates highly fine-grained descriptions and accurately captures the visual attributes of each instance.

However, due to the inherent limitations of textual representations, these captions still struggle to precisely encode, or to effectively guide the text encoder to understand, spatial relations, inter-instance interactions, and other more complex relationships. Moreover, because the instance captioner is essentially an MLLM, translating its internal text-visual alignment back into textual form and then feeding this text again into the video diffusion model’s text encoder may introduce information loss and cumulative errors.

Since the Open-Sora model allows specifying a motion score, we additionally generate three sets of videos under different motion-score settings. We observe that higher motion scores indeed lead to videos with noticeably larger motion ranges. Nevertheless, across both test cases, all three generated versions exhibit varying degrees of missing-instance issues. Although this might

be partially attributed to the reduced spatial resolution, our hardware constraints prevent us from isolating this factor.

9.4. Evaluation on More Metrics and Benchmarks

Due to space limitations in the main text, we provide *additional experiments* here based on several widely recognized metrics and benchmarks for video generation, briefly introducing the different metrics and benchmarks, and recording as well as analyzing the experimental results.

VideoScore VideoScore [13] is a learned, fine-grained evaluation metric designed to approximate human feedback on video generation quality. It is trained on the VideoFeedback dataset, which contains tens of thousands of human-annotated videos rated across multiple dimensions, including visual quality, temporal consistency, dynamic richness, text-to-video alignment, and factual consistency. The resulting metric can generate scalar feedback scores for each dimension, providing a multi-faceted, human-aligned signal that correlates strongly with human judgments. Unlike simple distributional metrics (such as FVD) or single-aspect scores, VideoScore enables more nuanced, aspect-specific evaluation of generative video models, making it particularly useful for optimizing models in a human-preference-aware manner. The VideoScore evaluation framework consists of two model versions and measures performance across five distinct dimensions. The detailed experimental results are presented in Table. 4 and Table. 5.

VBench-Series To enable comprehensive and standardized for video generation, the VBench-series of benchmarks provides a progressively refined suite of evaluation tools tailored for modern video generation systems. (1) *VBench* [21] introduced the first

Caption

The setting sun casts a warm glow over turquoise ocean waves breaking against a rocky cliff with white buildings and evergreen trees on it. Three sailboats navigate the calm waters near a sandy beach with a metal railing in the foreground.



Instance Captioner

A sailboat, with a white hull and a single mast, stays at the bottom-right, moving gently through the water. Another sailboat, also white with a mast and sails, remains at the bottom-right, appearing stationary. A third sailboat, with a white hull and sails, moves from the bottom-middle to the bottom-right, sailing smoothly on the blue expanse. The scene is a tranquil seascape at sunset, with a rocky island featuring white buildings and greenery, and a clear sky with a few birds flying. The camera movement is a slow pan to the left, capturing a wide view of the ocean and the rocky island, creating a serene and picturesque atmosphere.

People walking on a stone bridge over a wide river, with trees and modern skyscrapers on its side. Boats move along the river under a sunny blue sky.



Instance Captioner

A man in a black suit and white shirt, positioned at the bottom-left, walks confidently with a relaxed posture and a watch on his left wrist. A woman, also at the bottom-left, wears a white floral dress and a red shoulder bag, her head turned slightly to the side as she enjoys the view. Another woman, dressed in a white shirt and black pants with a panda bear backpack, stands still at the bottom-middle, her arms crossed and a neutral expression facing away from the camera. The scene is a picturesque urban landscape with a wide, calm river flowing gently. On one side of the river, modern skyscrapers rise high into the sky, their glass facades reflecting the sunlight. Trees line the riverbank, adding a touch of greenery to the sleek and elegant cityscape. The overall atmosphere is serene and tranquil, with a gentle and soothing presence. The camera movement is a slow pan to the right, capturing a wide-angle view of the city skyline, providing a stunning and serene perspective of the urban landscape.

Video Output



motion score = 1



motion score = 4



motion score = 7



motion score = 1



motion score = 4



motion score = 7

Figure 6. Generated results of InstanceCap, showing the original captions and the captions processed by the instance captioner. We also present the outputs from Open-Sora under different motion score settings, visualizing the first, middle, and last frames.

large-scale, multi-dimensional evaluation protocol specifically designed for video diffusion and autoregressive generators. Instead of relying solely on traditional metrics such as FVD or IS, VBench organizes evaluation into multiple capability dimensions, including *appearance quality*, *motion consistency*, *temporal coherence*, *subject identity preservation*, and *text-video alignment*. It further provides human-annotated references and model-predicted proxies, enabling both automated and human-aligned scoring. (2) *VBench++* [22] builds upon VBench by *adding evaluations for I2V models*. More importantly, VBench++ introduces an assessment of *generative models' trustworthiness*, specifically measuring: how well they generate content that is fair across different cultures and demographics, and how effectively they avoid producing harmful or offensive content. and demographics, and how

effectively they avoid producing harmful or offensive content. (3) *VBench2* [51] further introduces evaluations of generative models' *intrinsic faithfulness*, such as whether the generated videos adhere to physical laws, commonsense reasoning, anatomical correctness, and compositional integrity.

Some of the metrics in VBench rely on predefined prompts and fixed evaluation criteria designed to provide a unified and deterministic benchmark for video generation models. However, such metrics are not suitable for instance-level evaluation. Therefore, we only include VBench metrics that support evaluating customized video outputs when comparing InstanceV with state-of-the-art models. In addition, since InstanceV is not specifically designed to generate videos containing humans, we exclude the ethics and fairness-related metrics in VBench++ as well as the

Methods	Resolution	Subject Consistency \uparrow	Background Consistency \uparrow	Dynamic Degree \uparrow	Aesthetic Quality \uparrow	Imaging Quality \uparrow	Multi-View Consistency \uparrow
Wan2.1	480P	0.97697	0.97170	0.14000	0.57583	0.73665	0.43970
Wan2.2	720P	0.95958	0.95592	0.20000	0.51785	0.71953	0.46638
HunyuanVideo	720P	0.96079	0.96021	0.57333	0.58501	0.69946	0.51205
CogVideoX	480P	0.98174	0.97467	0.20667	0.57144	0.68036	0.61747
SkyReelsV2	540P	0.96392	0.96650	0.34000	0.60456	0.69523	0.41249
InstanceV(ours)	480P	0.97237	0.97779	0.46000	0.60777	0.73499	0.55084
	720P	0.98211	0.97250	0.26000	0.57318	0.73875	0.62819

Table 6. Quantitative comparison of our proposed InstanceV with state-of-the-art video diffusion models using selected applicable metrics of *VBench*(first five) and *VBench2*(last one).

human-centric metrics in *VBench2*. Beyond the results reported in the main text, we further evaluate six metrics in total: *five quality-related metrics from VBench and one additional metric from VBench2*.

The experimental results are summarized in Table 6. Except for the *Dynamic Degree* metric, InstanceV outperforms all existing state-of-the-art models across the remaining metrics. For *Dynamic Degree*, HunyuanVideo achieves the best score, though this comes at the cost of weaker performance in *Subject Consistency* and *Background Consistency*. Our observations confirm that HunyuanVideo indeed produces videos with larger motion amplitudes. Overall, InstanceV demonstrates a more balanced and superior performance across diverse metrics, achieving a better trade-off between motion magnitude and temporal coherence, while also delivering stronger aesthetics and visual quality. In addition, for the *Multi-View Consistency* metric, InstanceV significantly surpasses most state-of-the-art models. CogVideoX shows comparable performance mainly because its generated videos contain fewer apparent camera-motion variations, making its multi-view consistency score closer to that of InstanceV.

10. More Details on Model Implementation

The notation below is kept consistent with the main text.

10.1. IMCA

For the visual tokens fed into the IMCA module, we fold them along the temporal dimension, as illustrated in Figure.2 of the main text. This design brings two major benefits:

- By folding the visual tokens along the temporal dimension, the instance prompt tokens are naturally folded as well. Consequently, the instance-level grounding information does not require temporal partitioning, making the IMCA design more concise and efficient.
- By folding visual tokens along the temporal dimension, the size of the attention map can be significantly reduced, which in turn decreases the computational overhead of the attention mechanism and relaxes the GPU memory and hardware requirements.

Moreover, since the native self-attention module primarily handles the modeling of spatial and temporal consistency, injecting instance-level grounding information separately for each frame does not significantly compromise the overall spatial-temporal coherence.

10.2. Attention Masks

To address the potential issue of small objects being overlooked, in addition to SAUG, we also experiment with using a *float-version attention mask*. Specifically, when a visual token corresponds to multiple instance tokens, we prioritize assigning higher attention weights to tokens corresponding to smaller instances. To implement this, we first sort the instance prompt tokens by their corresponding instance areas in descending order, and then modify the attention mask in MIV-CA to a floating-point version as follows:

$$M_{(i,j)}^t = \begin{cases} j \times \text{MaskBase} & \text{if } [V_i^t, I_j^t] = 1, \\ -\text{inf} & \text{if } [V_i^t, I_j^t] = 0, \end{cases}$$

, here *MaskBase* is a predefined positive constant, whose magnitude determines the scaling factor applied to the attention map. In practice, we find that values such as 0.1 and 0.01 are sufficient to achieve the desired effect. However, *MaskBase* may vary across different DiT-based video diffusion models, depending on the specific outputs and intermediate statistical information of each model’s DiT blocks.

10.3. STAPE

As illustrated in Figure. 5, when using the flow-match scheduler, different DiT blocks perform entirely different functions across timesteps. We observe that for most of the forward process, at timestep = 984, the output of the last DiT block already exhibits reasonably clear semantic structure, although the fine details are still incomplete. However, over many subsequent timesteps, the outputs of the other DiT blocks, except for the final one, still lack explicit semantic meaning. We attribute this to the different influences exerted on visual tokens by self-attention, which models spatial-temporal consistency, and cross-attention, which establishes text-visual alignment.

Therefore, assigning an adaptive instance-level global semantic enhancement to different DiT blocks at different timesteps can positively impact both the spatial-temporal consistency within visual tokens and the alignment between text and visual representations.

10.4. SAUG

When implementing SAUG, we compare *two reasonable design choices*. During unconditional forward passes, instance prompts must be left empty. However, simply replacing instance prompts

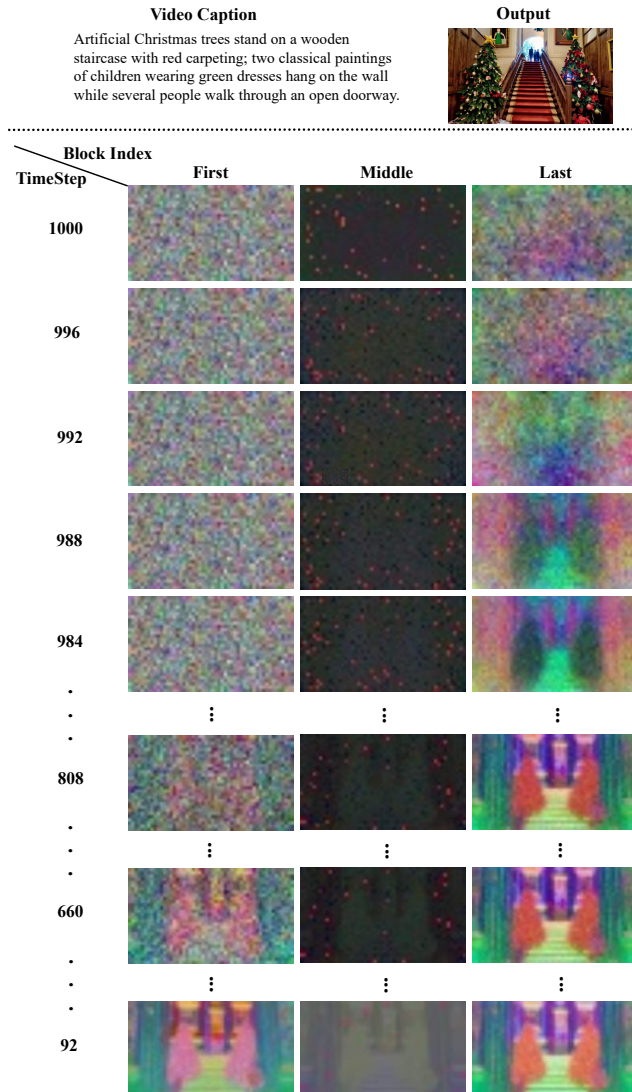


Figure 7. PCA visualization of the visual tokens produced by different backbone native DiT blocks at various timesteps. For illustration purposes, only the first $H \times W$ visual tokens are used.

with empty strings is ineffective: the attention mask would provide *no* positional guidance because all instance-prompt tokens and padding tokens collapse to identical embeddings. As a result, the projected value tokens become indistinguishable, and the output of the attention operation remains the same regardless of whether the attention mask is applied.

To ensure that the attention mask can meaningfully guide spatial positions, each instance prompt must be assigned an embedding that carries no explicit semantics but remains distinguishable across instances. We consider two practical solutions: (1) Extending the vocabulary of the native text encoder. We can expand the backbone’s tokenizer and embedding matrix to include additional placeholder tokens. Since the entire text encoder is frozen, these embeddings must be randomly initialized (e.g., using Xavier initialization [10]). (2) Reusing predefined special tokens in the

text encoder. Many pretrained text encoders define special tokens such as $\langle \text{bos} \rangle$, $\langle \text{eos} \rangle$, or the $\langle \text{extra_idx} \rangle$ tokens in models like uMT5 [45]. These tokens typically number in the dozens or even around one hundred, sufficient to cover the maximum number of instances in a single training video. Reusing $\langle \text{extra_idx} \rangle$ avoids modifying the tokenizer or embedding layer, and these tokens naturally provide semantically meaningless yet mutually distinguishable embeddings, making them ideal for representing different instances.

11. Potential Limitations and Future Study

11.1. Instance-level Grounding Information

One potential limitation of InstanceV lies in the relatively limited forms of instance-level grounding information it currently supports. At present, it only accommodates bounding-box-based spatial configurations and text-prompt-based instance attributes. Due to the computationally intensive nature of training and inference in video diffusion models, we primarily focused on designing a lightweight architecture to achieve effective instance-level grounding under a limited computational budget. We have already initiated preliminary investigations to extend this capability, but due to space constraints, these are not discussed in detail in the main text. Building upon frameworks such as GLIGEN [25] and InstanceDiffusion [40], it is possible to further enrich instance-level grounding information. For example, instance attributes need not be restricted to textual descriptions; more detailed guidance could be provided via a reference image or even a short video. Similarly, for spatial configurations, more precise and dedicated trajectory and motion information could be incorporated.

11.2. Acceleration

Building on InstanceV, we can further optimize computational efficiency. The IMCA module may not be required in every DiT block, as our experiments indicate that the overall video layout is largely established within the first few denoising timesteps. Therefore, IMCA can be omitted in later blocks without significant impact.

As shown in Figure 7, the output of the last DiT block stabilizes in terms of semantic content after timestep = 984, although the outputs of the preceding DiT blocks still lack clearly defined semantics for several subsequent timesteps. This observation motivates us to consider two directions: (1) whether we can perform a statistical analysis of the visual token outputs at each timestep under different video captions in existing video diffusion models, thereby establishing an efficient routing strategy that allows visual tokens, video captions, and instance-level grounding information to interact at the most effective timesteps and DiT blocks; (2) whether we can design a direct and efficient instance-level information exchange mechanism based on the interaction between native self-attention and native cross-attention, aiming to minimize potential conflicts between the two while preserving the quality of the outputs.

Furthermore, in the multi-head attention mechanism [37], different attention heads [9, 26] contribute unequally to the final output. As shown in Figure 9, the native self-attention modules in different DiT blocks exhibit substantial variation in their attention maps across different time steps, indicating that sharing across

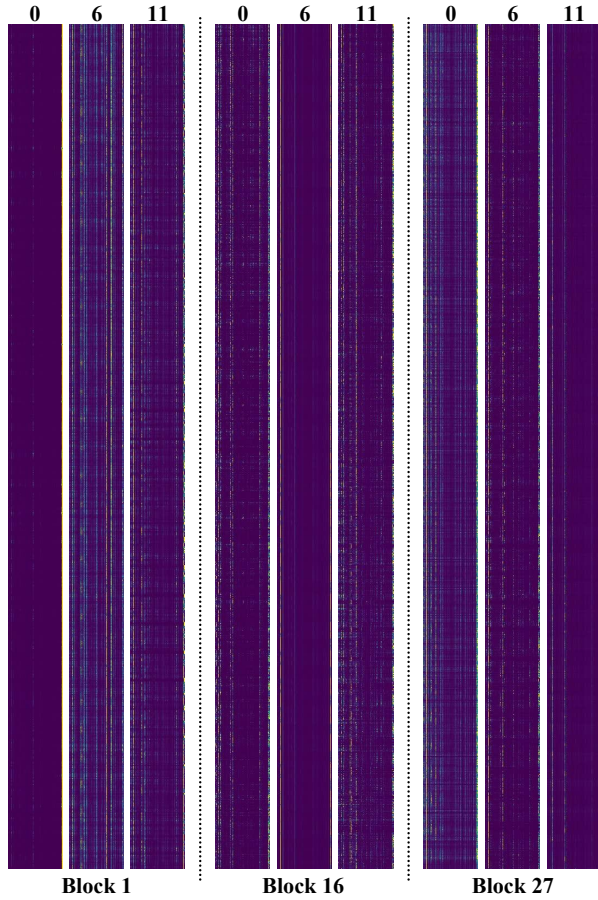


Figure 8. Visualization of the attention maps from different attention heads in the native cross-attention modules across various DiT blocks at timestep = 984. Padding tokens are omitted.

the final output is inherently imbalanced. Some attention maps capture strong semantic information, such as spatial or temporal cues, while others primarily reflect simple “self-focused” patterns. A similar phenomenon also appears in the native cross-attention modules, as illustrated in Figure 8. Due to space limitations, we only present the attention maps of different heads within the cross-attention modules across various DiT blocks at timestep = 984. We remove all attention maps corresponding to padding tokens and retain only the semantically meaningful regions.

This suggests a potential direction to selectively prune or allocate IMCA and cross-attention heads in each DiT block, enabling further computational acceleration [42, 49].

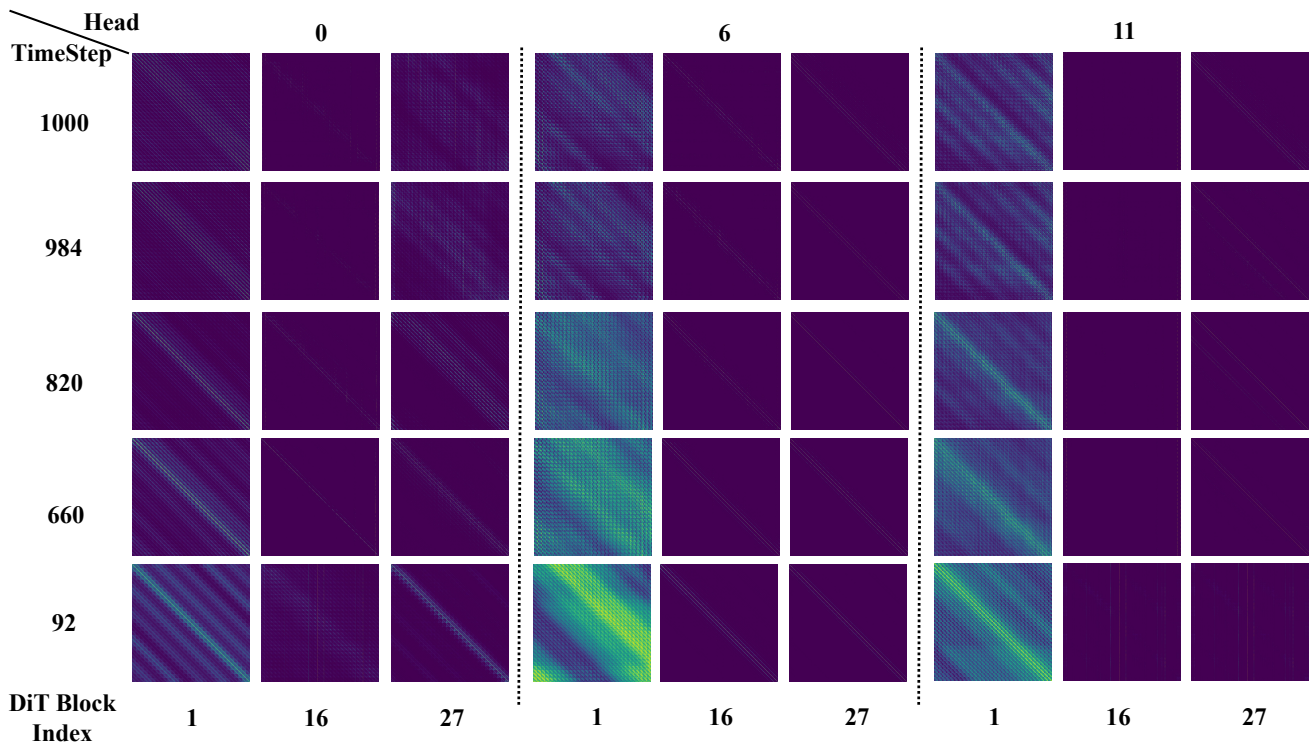


Figure 9. Visualization of attention maps after normalization from different heads within various DiT blocks at different timesteps in the native self-attention module.